

Accepted Manuscript

Discovery of 2-Pyridone Derivatives as Potent HIV-1 NNRTIs Using Molecular Hybridization Based on Crystallographic Overlays

Wenmin Chen, Yingshan Han, Peng Zhan, Diwakar Rai, Erik De Clercq, Christophe Pannecouque, Jan Balzarini, Zhongxia Zhou, Huiqing Liu, Xinyong Liu

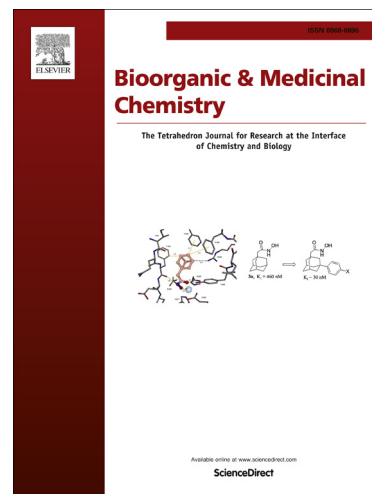
PII: S0968-0896(14)00091-1
DOI: <http://dx.doi.org/10.1016/j.bmc.2014.01.054>
Reference: BMC 11385

To appear in: *Bioorganic & Medicinal Chemistry*

Received Date: 7 December 2013
Revised Date: 24 January 2014
Accepted Date: 27 January 2014

Please cite this article as: Chen, W., Han, Y., Zhan, P., Rai, D., De Clercq, E., Pannecouque, C., Balzarini, J., Zhou, Z., Liu, H., Liu, X., Discovery of 2-Pyridone Derivatives as Potent HIV-1 NNRTIs Using Molecular Hybridization Based on Crystallographic Overlays, *Bioorganic & Medicinal Chemistry* (2014), doi: <http://dx.doi.org/10.1016/j.bmc.2014.01.054>

This is a PDF file of an unedited manuscript that has been accepted for publication. As a service to our customers we are providing this early version of the manuscript. The manuscript will undergo copyediting, typesetting, and review of the resulting proof before it is published in its final form. Please note that during the production process errors may be discovered which could affect the content, and all legal disclaimers that apply to the journal pertain.



Discovery of 2-Pyridone Derivatives as Potent HIV-1 NNRTIs Using Molecular Hybridization Based on Crystallographic Overlays

Wenmin Chen ^a, Yingshan Han ^b, Peng Zhan ^a, Diwakar Rai ^a, Erik De Clercq ^c,
Christophe Pannecouque ^c, Jan Balzarini ^c, Zhongxia Zhou ^a, Huiqing Liu ^a, Xinyong
Liu ^{a, *}

^aDepartment of Medicinal Chemistry, Key Laboratory of Chemical Biology (Ministry of Education), School of Pharmaceutical Sciences, Shandong University, No.44, West Culture Road, 250012, Jinan, Shandong, P.R. China

^bMcGill University AIDS Centre, Lady Davis Institute for Medical Research, Jewish General Hospital, Montreal, Quebec, Canada

^cRega Institute for Medical Research, KU Leuven, Minderbroedersstraat 10, B-3000 Leuven, Belgium

Abstract:

Based on crystallographic overlays of the known inhibitors TMC125 and R221239 complexed in RT, we designed a novel series of 4-phenoxy-6-(phenylamino)pyridin-2(1*H*)-one derivatives as HIV NNRTIs by molecular hybridization approach. The biological testing results indicated that 2-pyridone scaffold of these inhibitors was indispensable for their anti-HIV-1 activity, and substitution of halogen at the 3-position of the 2-pyridone ring would decrease the anti-HIV activity. Four most potent compounds had anti-HIV-1 III_B activities at low micromolar concentrations (EC₅₀=0.15-0.84 μM), comparable to that of nevirapine and delavirdine. Some compounds were selected to test their anti-HIV-1 RT inhibitory action and to perform molecular modeling studies to predict the binding mode of these 2-pyridone derivatives.

Keywords: NNRTIs, HIV, Drug design, 2-Pyridone, Molecular hybridization, Docking.

*Corresponding author: Tel.: +86-531-88382005; Fax: +86-531-88382731; E-mail address: xinyongl@sdu.edu.cn (X. Liu).

1. Introduction

In the life cycle of human immunodeficiency virus type 1 (HIV-1), reverse transcriptase (RT) is responsible for the conversion of single-stranded viral RNA into double-stranded proviral DNA, a prerequisite for integration into host DNA¹. Due to its important role in the HIV-1 life cycle, RT has been identified as a prime target for anti-HIV drug discovery. Among currently available RT inhibitors, non-nucleoside reverse transcriptase inhibitors (NNRTIs) hamper the polymerase activity of HIV RT through allosterically binding to the NNRTI-binding pocket (NNIBP) to distort the precise geometry of the DNA polymerase catalytic site^{2,3}. Because of their excellent antiviral potency, high specificity and low toxicity^{4,5}, NNRTIs have become the important ingredients of highly active antiretroviral therapy (HAART)⁶. However, due to the infidelity of HIV-1 RT during replication⁷, the emergence of RT mutations (especially K103N and Y181C) rapidly develop resistance to the first-generation NNRTIs with rigid structures, such as nevirapine (NVP) and efavirenz (EFV)⁸. In an effort to address the low resistance barrier issue, next generation NNRTIs have been designed with the structural feature of smaller building blocks connected by flexible linkers. Representative second generation of NNRTIs with improved drug resistance profiles are the recently marketed diarylpyrimidine analogues (DAPYs)⁹, rilpivirine (TMC278, RPV) and etravirine (TMC125, ETR) (Fig. 1)¹⁰⁻¹². However, there is still a need to explore novel NNRTIs to address the current issues of side effects, poor solubility, cross-resistance, and virologic failure, accompanied by the current NNRTI therapy¹³⁻¹⁷.

<Fig.1.>

Herein, we decided to employ TMC125 as an appropriate starting point for development of novel NNRTIs. After extensive literature survey, we focus our attention on a more recent second-generation congener, *viz.* 3-iodo-4-phenoxy pyridinone (IOPY) analogue R221239, which serves as a promising drug candidate due to its excellent profile of resilience to the most common resistance mutations¹⁸⁻²¹. The co-crystal structure of R221239 (2BE2)²² bound in the NNRTI pocket was overlaid with the published structure of RT-TMC125 complex (3MEC)²³, which demonstrated striking similarities in the geometry of the two bound inhibitors. It was indicated that TMC125 and R221239 shared some common

pharmacophoric features, viz. an aromatic ring (A) to develop π - π stacking interactions with the residues of W229, Y181 and Y188, a central heterocycle (C) with hydrogen bond donor and acceptor to participate in hydrogen bondings with the back bone of the residues K101/K103, and one hydrocarbon-rich region (B) to involve in hydrophobic contacts with the tolerant region of RT.

<Fig.2.>

Based on above pharmacophoric analysis and the crystallographic overlap studies, we designed a novel series of 4-phenoxy-6-(phenylamino)pyridin-2(1*H*)-one derivatives through combining the privileged structural features of TMC125 and R221239 using molecular hybridization²⁴ (Fig. 3): i) Replacing the central pyrimidine ring of TMC125 with the 2-pyridone ring, which was expected to serve both as hydrogen bond donor and acceptor. Meanwhile, halogen atoms were introduced to the 3-position of the 2-pyridone ring to evaluate their impacts on antiviral activity; ii) Fragment switching of the 2-aniline group and the 6-phenoxy group in TMC125 to the novel 2-pyridone template and modifying the substituents at the two phenyl rings. The yielded hybrid compounds are expected to maintain pre-selected characteristics of the original templates. Herein, we described the synthesis and the biological evaluation of these novel hybrid 2-pyridone derivatives as potent HIV NNRTIs. The structure and activity relationship (SAR) analysis and molecular modeling studies for these compounds will also be presented.

<Fig.3.>

2. Results and Discussion

2.1 Chemistry

The synthetic route of 4-phenoxy-6-(phenylamino)pyridin-2(1*H*)-one derivatives is outlined in Scheme 1. First, treatment of commercially available 2,6-dichloropyridine (**1**) with 30% aqueous H₂O₂ solution in CF₃COOH provided intermediate 2,6-dichloropyridine-1-oxide (**2**), which followed by chlorination with POCl₃ to afford 2,4,6-trichloro pyridine (**3**)²⁵. Then, **3** was selectively substituted by different phenols at C-4 position in the presence of K₂CO₃ to produce 2,6-dichloro-4-phenoxy pyridine intermediates **4(a-d)**²⁶, which was subsequently alcoholized by methanol in the presence of sodium methoxide to give intermediate **5(a-d)** in good yields (50-78%). Then, intermediate **5(a-d)** underwent Pd(OAc)₂ catalyzed cross-coupling reaction with corresponding phenylamines to provide

2-methoxypyridine compounds **6(a-f)** (62-76%).

Subsequently, the precursor compounds **6(a-f)** were converted to 4-phenoxy-6-(phenylamino)pyridin-2(1*H*)-one compounds **7(a-f)** using sodium iodide and chlorotrimethylsilane under reflux condition with good yields (76%-86%). Finally, halogenation at the 3-position of 2-pyridone derivatives **7(c-f)** with *N*-iodosuccinimide (NIS), *N*-bromosuccinimide (NBS), or *N*-chlorosuccinimide (NCS) respectively, afforded corresponding 3-halogenated-2-pyridone compounds **8(c-f)** in 25–50% yields²⁷.

<Scheme 1.>

2.2 Biological Activity

The synthesized compounds were evaluated for their anti-HIV activity in MT-4 cell cultures infected with wild-type HIV-1 strain (III_B), double mutant HIV-1 strain RES056 (K103N+Y181C), and HIV-2 strain (ROD), respectively. FDA-approved drug nevirapine (NVP) and delavirdine (DLV) were used as reference drugs for comparison. The biological results are represented as EC₅₀ values (anti-HIV activity), CC₅₀ values (cytotoxicity) and SI values (selectivity index, given by the CC₅₀/EC₅₀ ratio) (Tables 1 and Table 2).

In total, 15 compounds were found to exhibit anti-HIV-1 III_B activity in lower micromolar range (EC₅₀ = 0.15-9.3 μM) with selectivity index (SI) values ranging from 5 to > 244. The most potent compound **7d** was found to prevent the cytopathic effect of HIV-1 III_B with an EC₅₀ value of 0.15 μM, less potent than TMC125 (EC₅₀ = 1.4 nM)^{28,29} and R221239 (EC₅₀ = 2.0 nM)²², but comparable to NVP (EC₅₀ = 0.18 μM) and superior to DLV (EC₅₀ = 0.91 μM). Additionally, none of these compounds was active against HIV-1 RES056 strain at subtoxic concentrations.

The contribution of the 2-pyridone scaffold to the biological activities was firstly assessed. As shown in Table 1, all the synthesized 2-pyridone compounds **7(a-f)** displayed improved anti-HIV-1 III_B activity and higher SI values as compared to corresponding 2-methoxy-pyridine analogues **6(a-f)**, which indicated that the 2-pyridone was an essential scaffold for these 2-pyridone inhibitors to exhibit anti-HIV-1 activity. Subsequently, to exploit the SAR features of R₂, we synthesized the 2-pyridone analogues **7(a-c)** which all bear a 2,4,6-trimethyl group (R₁) on the A-ring and only differ in the R₂ substitution on the B-ring. The biological results

showed that the 2-pyridone compound **7c** ($EC_{50} = 0.37 \mu\text{M}$) with a 4-cyano group (R_2) on the B-ring was about 4-fold more active than the corresponding compounds bearing a 4-methyl group (**7b**, $EC_{50} = 1.4 \mu\text{M}$) or a 4-nitro group (**7a**, $EC_{50} = 1.4 \mu\text{M}$), which suggested that the 4-cyano group was the optimal substituent on the B-ring, but more studies are required to confirm this hypothesis (Table 1).

< Table 1.>

Next, keeping the most optimal cyano group as R_2 substituent on the B-ring, different R_1 substituents were introduced on the A-ring of these 2-pyridone analogues (Table 2). Comparing the EC_{50} and CC_{50} values of 2-pyridone derivatives **7(c-f)**, we found that compound **7d** bearing a 4-cyano-2,6-dimethyl-substituent on the A-ring possessed better activity and a higher SI value than the compounds with a 2,4,6-trimethyl group (**7c**), 2,6-dimethyl group (**7e**), or 3,5-dimethyl substitution pattern (**7f**) (Table 1). It was noteworthy that introduction of a 3,5-dimethyl group in the A-ring furnished compound **7f** devoid of any anti-HIV-1 activity, whereas this group was identified as an optimal substituent for IOPY analogues. It appeared that the *meta*-position of the A-ring was located in a sterically unfavorable region while the *ortho*-/*para*- positions of the A-ring were favorable to introduce substitutions. Therefore, the substitution patterns on the A-ring (left wing) of these 2-pyridone compounds was in agreement with that of DAPYs, but different from that of IOPYs.

Finally, different halogen atoms were introduced into the 3-position of the 2-pyridone compounds **7(c-f)** respectively to investigate their influence on antiviral activity (Table 2). According to the reported literatures^{22, 30}, the iodine atom at the 3-position of the lead R221239 could develop an electrostatic interaction with the Y188 carbonyl oxygen, which greatly contributed to its binding affinity with RT. Inspired by this finding, an iodine atom was firstly introduced to the 3-position of the newly designed 2-pyridone compounds **7(c-f)** to explore whether it would contribute to their biological activity as it did in R221239^{22, 31}. However, all the 3-iodo substituted 2-pyridone compounds (**8c1**, **8d1**, **8e1**) (Table 2) exhibited decreased anti-HIV-1 (III_B) activities than the corresponding 3-unsubstituted 2-pyridone compounds (**7c**, **7d**, **7e**) (Table 1). The discrepancy between the SARs of IOPYs and these newly developed 2-pyridone derivatives indicated that the latter may bind to RT in a mode different from IOPYs. Additionally, the crystallographic overlay studies (Fig. 1) demonstrated

that the 3-iodo group of the pyridone moiety in R221239 generally overlapped with the 5-bromo group of pyrimidine in TMC125. Therefore, the bromo atom was also introduced into the 3-position of the 2-pyridone, for comparison, as well as the chloro atom, generating eight compounds (**8c2**, **8c3**, **8d2**, **8d3**, **8e2**, **8e3**, **8f2**, and **8f3**). Unfortunately, all these 3-bromo/choloro substituted 2-pyridone compounds were not superior to corresponding unsubstituted analogues **7(c-f)** and 3-iodio substituted analogues (**8c1**, **8d1**, **8e1**). These resulted revealed that substituents (X) at the 3-position of the 2-pyridone ring contributed to the antiviral activities in the following order (of decreasing activity): H > I > Br and Cl.

<Table 2.>

In summary, preliminary SAR studies of these novel 4-phenoxy-6-(phenylamino)pyridin-2(1*H*)-one derivatives revealed the important structural requirements to maintain high potency against HIV-1 virus: i) the optimal moiety for the left wing (A-ring) was a 4-cyano-2,6-dimethylphenxoy group; ii) the best group for the right wing (B-ring) was a 4-cyanophenylamino group; iii) 3-unsubstituted-2-pyridone derivatives were superior to 3-halogenated-2-pyridone analogues.

In addition, all the title compounds were also evaluated for their capability to inhibit the HIV-2 replication in MT-4 cells, but none was found effective at test concentration, indicating that newly developed compounds were only specific for HIV-1 (Supplementary materials).

2.3 Inhibition of HIV-1 RT

To confirm the drug target of these 2-pyridone inhibitors, two compounds (**7d** and **7c**) with the highest potency were evaluated for their HIV-1 RT inhibitory, using a Roche RT kit. The colorimetric of the RT assay takes advantage of the ability of RT to synthesize the DNA, starting from the template/primer hybrid poly(A) × oligo(dT)₁₅. The detection and quantification of the synthesized DNA as a parameter for RT activity follows a sandwich ELISA protocol (as descibled in the Kit): Biotin-labeled DNA binds to the surface of microplate (MP) modules that have been precoated with streptavidin. In the next step, an antibody to digoxigenin, conjugated to peroxidase (anti-DIG-POD), binds to the digoxigenin-labeled DNA. In the final step, the peroxidase substrate ABTS is added. The peroxidase enzyme catalyzes the cleavage of the substrate, producing a colored reaction product. The absorbance of the

samples was determined using a microplate (ELISA) reader and was directly correlated to the level of RT activity in the sample.

The results showed that the anti-RT activity of **7d** was comparable to that of NVP, but lower than that of ETR. Another compound **7c** was less potent than both ETR and NVP (Table 3). The biological results proved that the newly discovered 2-pyridone derivatives displayed anti-HIV-1 activity by inhibiting RT, and belonged to HIV-1 NNRTIs.

<Table 3.>

2.4 Molecular modeling analysis

Molecular docking using surflex-dock module of Sybyl-X 1.1 was performed to predict the binding mode of the representative 2-pyridone inhibitors (**7d** and **8d1**) with RT and to rationalize the results of SAR studies. Coordinates of the NNIBP were taken from the crystal structure of the RT/TMC125 complex (PDB code: 3MEC) due to the high degree of structural similarity between TMC125 and the newly designed 2-pyridone compounds. This program docks a ligand automatically into the binding site of a receptor, using a protomol-based method and an empirically derived scoring function. The root-mean-square deviations (RMSD) value for the re-dock result of bound ligand TMC-125 is 0.4320 Å, indicative of that this docking program is reliable and accurate.

The highest-scored docking conformation of **7d** at the binding site of RT was displayed in overlap with the crystallized position of TMC125 (blue) by PyMOL version 1.5 (<http://www.pymol.org/>). Inspection of the binding conformation of **7d** revealed a fair superposition to that of TMC125 (Fig. 4). The central ring of **7d** was orientated by dual hydrogen bonds between the CONH moiety of the 2-pyridone with the back bone C=O and NH of K101, respectively. Indeed, according to the biological results, replacement of the 2-pyridone ring with 2-methoxypyridine decreased the anti-HIV-1 activity (Table 1), which proves the importance of the central 2-pyridone ring for interactions with RT. A third hydrogen bond between the NH group of the 4-cyano phenylamino moiety with K101 was observed. Additionally, the benzonitrile moiety of **7d**, which overlapped with the right ring of TMC125, was located in a hydrophobic channel surrounded by P236, V106 and Y318. The dimethylcyanophenyl of **7d** developed favorable face-to-face π - π interactions with the aromatic rings of Y181 and Y188. It is noteworthy that the orientation of the dimethylcyanophenyl group of **7d** was slightly different from that of TMC125. This conformational

perturbation may reduce the tight contact of the dimethylcyanophenyl group with the conserved residue W229, which may explain the low sensitivity of compound **7d** to the drug-resistant HIV-1 strain (RES056 strain: K103N+Y181C).

<Fig. 4.>

Introduction of an iodine atom at the 3-position of **7d** yielded the less active compound **8d1**. We found that the distance between the iodine atom of **8d1** with the C=O of Y188 (6.04 Å) was beyond the minimal van der Waals contact distance (3.55 Å), which may explain why the iodine atom of **8d1** did not contribute to the protein-ligand binding affinity as it did to IOPYs^{21,22}. Instead, the steric hindrance of the iodine atom pushed **8d1** to move towards the bottom of the binding pocket, which disrupted the dual hydrogen bonds between the CONH moiety of the 2-pyridone with the back bone of K101 (Fig. 5). The absence of the multiple hydrogen bonds weakened the binding affinity of **8d1**, which may ultimately lead to the 19-fold lower activity of **7d1** (EC₅₀ = 2.9 μM) than that of **7d** (EC₅₀ = 0.15 μM) (Fig. 5).

<Fig. 5.>

The docking studies revealed the binding orientation of these 2-pyridone derivatives and provided critical insights for further development of these compounds.

3. Conclusion

In summary, we designed a series of 4-phenoxy-6-(phenylamino)pyridin-2(1*H*)-one derivatives as potent HIV-1 NNRTIs using molecular hybridization based on crystallographic overlay studies of the lead compounds TMC125 and R221239. The biological assay showed that 15 compounds exhibited significant potency against wild-type HIV-1 strain (III_B) at micromolar concentrations (EC₅₀ = 0.15-9.3 μM). Among them, compound **7d** displayed the highest activity with an EC₅₀ value of 0.15 μM and SI of 166, providing a good starting point for further structural optimization. Additionally, the molecular modeling studies of representative 2-pyridone inhibitors with RT revealed that these inhibitors adopt a similar binding mode with TMC125. Further efforts to improve the antiviral activity of these 2-pyridone typed NNRTIs by rational design to improve their drug resistance profiles and water solubility are currently underway and will be reported in due course.

4.1 Experimental Section

4.1. Chemistry

Mass spectrometry was performed on an API 4000 triple-quadrupole mass spectrometer (Applied Biosystems/MDS Sciex, Concord, ON, Canada). IR spectra were recorded with Nicolet-6700 model FT-IR spectrometer (Thermo Scientific, Waltham, MA, USA) using KBr pellets. $^1\text{H-NMR}$ and $^{13}\text{C-NMR}$ spectra were recorded on a Bruker Avance DRX 600 spectrometer (Bruker, Fällanden, Switzerland), Bruker AV-400 spectrometer (Bruker BioSpin, Switzerland), or Bruker AVANCE-300 spectrometer (Bruker BioSpin, Switzerland), using solvents as indicated (CDCl_3 or $\text{DMSO-}d_6$). Chemical shifts were reported in δ values (ppm) with tetramethylsilane as the internal reference, and J values were reported in hertz (Hz). Melting points (mp) were determined on a micromelting point apparatus (Tian Jin Analytical Instrument Factory, Nankai, Tianjin, China). Flash column chromatography was performed on columns packed with silica gel 60 (200–300 mesh) (Qingdao waves silica gel desiccant co., Ltd, Qingdao, China). Thin layer chromatography was performed on pre-coated HUANGHAI® HSGF254, 0.15-0.2 mm TLC-plates (Yantai Jiangyou Silica Gel Development Co., Ltd., Yantai, Shandong, China). Solvents (Tianjin Fuyu Fine Chemical Co., Ltd., Wuqing, Tianjin, China) were of reagent grade and were purified and dried by standard methods when necessary. The key reactants including 2,6-dichloropyridine, $\text{Pd}(\text{OAc})_2$, XantPhos, chlorotrimethylsilane, *N*-iodosuccinimide NIS, *N*-bromosuccinimide NBS and *N*-chlorosuccinimide NCS, *etc.* were purchased from Adamas-beta Co. Ltd (Shanghai, China).

4.1.1. General procedure for synthesis of 2,6-dichloropyridine-1-oxide (2)

A solution of 2,6-dichloropyridine (**1**) (10.0 g, 0.067 mol) in a mixture of CF_3COOH (80 mL) and 30% aq. H_2O_2 (25 mL) was heated at reflux for 3h. Then, saturated $\text{Na}_2\text{S}_2\text{O}_4$ solution was added to the mixture until hydrogen peroxide was consumed completely *via* an inspection with potassium iodide-starch test paper. Thereafter, the reaction mixture was concentrated under reduced pressure to about 10 mL and then poured on 50 mL water. The unreacted 2,6-dichloropyridine (**1**) was formed as a precipitate and was then removed by filtration. The filtrate was basified by addition of solid Na_2CO_3 , causing the precipitation of a white solid, which was filtered and dried, giving the crude 2,6-dichloropyridine-1-oxide (**2**) as a white solid, yield 55%, mp: 137-138°C.

4.1.2. General procedure for synthesis of 2,4,6-trichloropyridine (3)

A mixture of 2,6-dichloropyridine-1-oxide (**2**) (8.20 g, 0.050 mol) in POCl₃ (25 mL) was refluxed for 4h. Then, the solvent was evaporated under reduced pressure. The residue was poured into crushed ice and extracted with petroleum ether (3×50 mL). The combined organic phase was dried over K₂CO₃, filtered, and concentrated *in vacuo*. The residue was further purified by flash column chromatography using ethyl acetate/petroleum ether as an eluent to give 2,4,6-trichloropyridine (**3**) as colorless needles, yield 85%, mp: 32-33°C.

4.1.3. General procedure for the synthesis of 2,6-dichloro-4-(phenoxy)pyridines **4(a-d)**

A mixture of different phenols (5.0 mmol) and K₂CO₃ (0.83 g, 6.0 mmol) in 15 mL DMF was stirred at room temperature for 15min. Then, 2,4,6-trichloropyridine (**3**) (0.91 g, 5.0 mmol) was added and the mixture as heated to 100°C under a nitrogen atmosphere. The reaction was followed by TLC until its completion. Then, the solvent was evaporated off and the residue, after addition of water, was extracted with ethyl acetate. The organic layer was dried over Na₂SO₄ and concentrated *in vacuo*. The residue was recrystallized from ethyl acetate and petroleum ether or purified by column chromatography using ethyl acetate and petroleum ether as an eluent to give **4(a-d)**.

4.1.3.1. 2,6-dichloro-4-(mesityloxy)pyridine (**4a**)

Colorless crystal, recrystallized from ethyl acetate and petroleum ether, yield: 85%, mp: 129-130°C; ¹H-NMR (400 MHz, CDCl₃) δ: 2.06 (s, 6H, CH₃), 2.31 (s, 3H, CH₃), 6.66 (d, *J* = 1.32 Hz, 2H, Py-*H*), 6.93 (s, 2H, Ph-*H*); ¹³C-NMR (100 MHz, CDCl₃) δ: 15.99, 20.79, 109.73, 129.94, 130.09, 136.17, 147.14, 151.68, 167.27; MS-ESI: 282.3 [M+H]⁺, 284.2 [M+H]⁺.

4.1.3.2. 2,6-dichloro-4-(4-cyano-2,6-dimethylphenoxy)pyridine (**4b**)

Colorless crystal, purified by column chromatography using ethyl acetate/petroleum ether (1:20) as an eluent, yield 68%, mp: 168-169°C; ¹H-NMR (400 MHz, CDCl₃) δ: 2.17 (s, 6H, CH₃), 6.65 (d, *J* = 1.32 Hz, 2H, Py-*H*), 7.48 (s, 2H, Ph-*H*); ¹³C-NMR (100 MHz, CDCl₃) δ: 16.12, 109.58, 110.78, 118.03, 132.58, 133.39, 152.11, 152.62, 165.72; MS-ESI: 293.4 [M+H]⁺, 295.3 [M+H]⁺.

4.1.3.3. 2,6-dichloro-4-(2,6-dimethylphenoxy)pyridine (**4c**)

Colorless crystal, recrystallized from ethyl acetate and petroleum ether, yield: 80%, mp: 86-87°C; ¹H-NMR (400 MHz, CDCl₃) δ: 2.11 (s, 6H, CH₃), 6.66 (d, *J* = 1.32 Hz, 2H, Py-*H*), 7.13-7.14 (m, 3H, Ph-*H*); ¹³C-NMR (100 MHz, CDCl₃) δ: 16.09, 109.73,

126.60, 129.54, 130.44, 149.31, 151.73, 166.99; MS-ESI: 268.3 [M+H]⁺, 270.4 [M+H]⁺.

4.1.3.4. 2,6-dichloro-4-(3,5-dimethylphenoxy)pyridine (**4d**)

Colorless crystal, purified by column chromatography using ethyl acetate/petroleum ether (1:30) as an eluent, yield 84%, mp: 200-201 °C; ¹H-NMR (400 MHz, CDCl₃) δ: 2.34 (s, 6H, CH₃), 6.69 (d, *J* = 1.32 Hz, 2H, Py-*H*), 6.76 (s, 2H, Ph-*H*), 6.94 (s, 1H, Ph-*H*); ¹³C-NMR (100 MHz, CDCl₃) δ: 21.30, 110.05, 118.33, 128.11, 140.59, 151.39, 153.00, 167.99; MS-ESI: 268.3 [M+H]⁺, 270.3 [M+H]⁺.

4.1.4. General procedure for the synthesis of 2-chloro-6-methoxy-4-phenoxy-pyridines **5(a-d)**

Intermediates **4(a-d)** (0.01 mol) were dissolved in MeONa/MeOH (prepared from 1.15 g Na and 20 mL MeOH) and the mixture was heated to reflux for 4h. Next, the solvent was evaporated off and the residue, after addition of water, was taken up in CH₂Cl₂. The combined organic layer was dried over Na₂SO₄. Evaporation of the solvent afforded 2-chloro-6-methoxy-4-phenoxy-pyridines **5(a-d)**.

4.1.4.1. 2-chloro-4-(mesityloxy)-6-methoxy-pyridine (**5a**)

White solid, yield 78%, mp: 98 °C; ¹H-NMR (400 MHz, CDCl₃) δ: 2.06 (s, 6H, CH₃), 2.29 (s, 3H, CH₃), 3.89 (s, 3H, OCH₃), 5.93 (d, *J* = 1.56 Hz, 1H, Py-*H*), 6.44 (d, *J* = 1.56 Hz, 1H, Py-*H*), 6.89 (s, 2H, Ph-*H*); ¹³C-NMR (100 MHz, CDCl₃) δ: 15.99, 20.77, 54.15, 94.02, 105.11, 129.80, 130.27, 135.56, 147.61, 149.53, 165.34, 167.72; MS-ESI: 278.3, 280.2 [M+H]⁺.

4.1.4.2 2-chloro-4-(4-cyano-2,6-dimethyl)-6-methoxyphenoxy-pyridine (**5b**)

White solid, yield 72%, MS-ESI: 289.3, 291.4 [M+H]⁺.

4.1.4.3 2-chloro-4-(2,6-dimethylphenoxy)-6-methoxy-pyridine (**5c**)

White solid, yield 72%, MS-ESI: 264.3, 266.4 [M+H]⁺.

4.1.4.4 2-chloro-6-methoxy-4-(3,5-dimethylphenoxy)-pyridine (**5d**)

White solid, yield 68%, MS-ESI: 264.2, 266.3 [M+H]⁺.

4.1.5. General procedure for the synthesis of 2-methoxy-pyridine compounds **6(a-f)**.

In a schlenk-type flask, corresponding phenylamine (0.01 mol) and intermediates **5(a-d)** (0.01 mol) were dissolved in dry dioxane (25 mL), and then Pd(OAc)₂ (67.3 mg, 0.3mmol), XantPhos (347.2 mg, 0.6 mmol) and NaO-*t*Bu (1.44 g, 0.015 mol) were added. The mixture was heated to 100 °C while stirring under a nitrogen atmosphere. The reaction was followed by TLC until its completion. After cooling, the solvent was evaporated under reduce pressure. The residue was purified by flash

column chromatography using ethyl acetate/petroleum ether as eluent to give compounds **6(a-f)**.

4.1.5.1. 4-(mesityloxy)-6-methoxy-N-(4-nitrophenyl)pyridin-2-amine (**6a**)

Yellow solid, yield 72%, mp: 197-199°C; ¹H-NMR (400 MHz, DMSO-*d*₆) δ: 2.05 (s, 6H, 2CH₃), 2.27 (s, 3H, CH₃), 3.89 (s, 3H, OCH₃), 5.81 (d, *J* = 1.64 Hz, 1H, Py-*H*), 5.86 (d, *J* = 1.44 Hz, 1H, Py-*H*), 7.01 (s, 2H, Ph-*H*), 7.84 (d, *J* = 9.32 Hz, 2H, Ph-*H*), 8.14 (d, *J* = 9.36 Hz, 2H, Ph-*H*), 9.80 (s, 1H, NH); ¹³C-NMR (100 MHz, DMSO-*d*₆) δ: 16.11, 20.81, 54.30, 88.65, 90.16, 117.18, 125.67, 130.13, 130.45, 135.31, 139.90, 147.90, 148.42, 154.63, 165.01, 167.57; ESI-MS: 380.5 [M+H]⁺.

4.1.5.2. 4-(mesityloxy)-6-methoxy-N-(*p*-tolyl)pyridin-2-amine (**6b**)

White solid, yield 70%, mp: 107-108°C; ¹H-NMR (400 MHz, CDCl₃) δ: 2.08 (s, 6H, 2CH₃), 2.27 (s, 3H, CH₃), 2.30 (s, 3H, CH₃), 3.83 (s, 3H, OCH₃), 5.48 (d, *J* = 1.60 Hz, 1H, Py-*H*), 5.91 (d, *J* = 1.60 Hz, 1H, Py-*H*), 6.25 (s, 1H, NH), 6.86 (s, 2H, Ph-*H*), 7.09 (d, *J* = 8.24 Hz, 2H, Ph-*H*), 7.21 (d, *J* = 8.36 Hz, 2H, Ph-*H*); ¹³C-NMR (100 MHz, CDCl₃) δ: 16.05, 20.75, 53.49, 86.37, 87.13, 120.42, 129.49, 129.63, 130.61, 132.07, 134.88, 148.11, 155.77, 165.21, 168.14; ESI-MS: 349.4 [M+H]⁺.

4.1.5.3. 4-((4-(mesityloxy)-6-methoxypyridin-2-yl)amino)benzotrile (**6c**)

White solid, yield 76%, mp: 198-200°C; ¹H-NMR (400 MHz, CDCl₃) δ: 2.09 (s, 6H, 2CH₃), 2.29 (s, 3H, CH₃), 3.89 (s, 3H, OCH₃), 5.70 (d, *J* = 1.52 Hz, 1H, Py-*H*), 5.91 (d, *J* = 1.48 Hz, 1H, Py-*H*), 6.66 (s, 1H, NH), 6.89 (s, 2H, Ph-*H*), 7.53 (s, 2H, Ph-*H*); ¹³C-NMR (100 MHz, DMSO-*d*₆) δ: 16.04, 20.78, 53.87, 88.63, 89.81, 103.35, 117.73, 119.61, 129.65, 130.51, 133.29, 135.24, 144.95, 147.90, 153.49, 165.22, 168.06; ESI-MS: 360.4, 362.4 [M+H]⁺.

4.1.5.4. 4-((2-((4-cyanophenyl)amino)-6-methoxypyridin-4-yl)oxy)-3,5-dimethylbenzotrile (**6d**)

White solid, yield 62%, mp: 229-230°C; ¹H-NMR (400 MHz, CDCl₃) δ: 2.18 (s, 6H, 2CH₃), 3.91 (s, 3H, OCH₃), 5.63 (d, *J* = 1.64 Hz, 1H, Py-*H*), 5.89 (d, *J* = 1.64 Hz, 1H, Py-*H*), 6.86 (s, 1H, NH), 7.41 (s, 2H, Ph-*H*), 7.55 (d, *J* = 8.84 Hz, 2H, Ph-*H*), 7.60 (d, *J* = 8.92 Hz, 2H, Ph-*H*); ¹³C-NMR (100 MHz, CDCl₃) δ: 16.10, 54.00, 88.31, 89.50, 103.62, 109.55, 117.96, 118.45, 119.53, 132.92, 133.12, 133.30, 144.78, 153.83, 153.93, 165.30, 166.57; ESI-MS: 371.4 [M+H]⁺.

4.1.5.5. 4-((6-methoxy-4-(2,6-dimethylphenoxy)-pyridin-2-yl)amino)benzotrile (**6e**)

White solid, yield 72%, mp: 159-160°C; ¹H-NMR (400 MHz, CDCl₃) δ: 2.13 (s, 6H, 2CH₃), 3.89 (s, 3H, OCH₃), 5.70 (d, *J* = 1.64 Hz, 1H, Py-*H*), 5.90 (d, *J* = 1.60 Hz, 1H, Py-*H*), 6.72 (s, 1H, NH), 7.07-7.08 (m, 3H, Ph-*H*), 7.52-7.53 (m, 4H, Ph-*H*); ¹³C-NMR (100 MHz, CDCl₃) δ: 16.11, 53.98, 88.53, 89.69, 103.60, 117.88, 119.54, 125.81, 129.09, 130.97, 133.32, 144.79, 150.10, 153.47, 165.13, 167.94; ESI-MS: 346.3 [M+H]⁺.

4.1.5.6. 4-((6-methoxy-4-(3,5-dimethylphenoxy)-pyridin-2-yl)amino)benzonitrile (**6f**)

White solid, yield 70%, mp: 150-152°C; ¹H-NMR (400 MHz, DMSO-*d*₆) δ: 2.29 (s, 6H, 2CH₃), 3.87 (s, 3H, OCH₃), 5.87 (d, *J* = 1.72 Hz, 1H, Py-*H*), 5.92 (d, *J* = 1.68 Hz, 1H, Py-*H*), 6.79 (s, 2H, Ph-*H*), 6.92 (s, 1H, Ph-*H*), 7.65 (d, *J* = 8.84 Hz, 2H, Ph-*H*), 7.80 (d, *J* = 8.80 Hz, 2H, Ph-*H*), 9.57 (s, 1H, NH); ¹³C-NMR (100 MHz, DMSO-*d*₆) δ: 21.24, 54.19, 89.63, 91.65, 101.65, 117.94, 118.83, 120.16, 127.34, 133.54, 140.20, 146.16, 154.27, 164.84, 168.24; ESI-MS: 346.3 [M+H]⁺.

4.1.6. General procedure for synthesis of the 2-pyridone compounds **7(a-f)**

chlorotrimethylsilane (2.72 g, 0.025 mol) was added to a suspension of **6(a-f)** (0.005 mol) and sodium iodide (3.75 g, 0.025 mol) in acetonitrile. This mixture was stirred at reflux. Upon completion of the reaction, the solvent was evaporated *in vacuo*. The residue was suspended in ethyl acetate, washed by 10% aq. Na₂S₂O₃ solution (10 mL). The precipitate was then filtered and recrystallized from methanol to give target compounds **7(a-f)**.

4.1.6.1. 4-(mesityloxy)-6-((4-nitrophenyl)amino)pyridin-2(1H)-one (**7a**)

Yellow solid, yield 85%, decomposed at 260°C; ¹H-NMR (400 MHz, DMSO-*d*₆) δ: 2.05 (s, 6H, CH₃), 2.27 (s, 3H, CH₃), 5.66 (s, 1H, Py-*H*), 5.74 (s, 1H, Py-*H*), 6.99 (s, 2H, Ph-*H*), 7.88 (d, *J* = 9.24 Hz, 2H, Ph-*H*), 8.10 (d, *J* = 9.52 Hz, 2H, Ph-*H*), 9.67 (s, 1H, NH), 10.59 (s, 1H, CONH); ¹³C-NMR (100 MHz, DMSO-*d*₆) δ: 16.13, 20.80, 88.01, 89.28, 117.08, 125.52, 130.07, 130.49, 135.18, 139.70, 147.95, 148.76, 154.63, 164.57, 167.67; ESI-MS: 366.4 [M+H]⁺.

4.1.6.2. 4-(mesityloxy)-6-(*p*-tolylamino)pyridin-2(1H)-one (**7b**)

White solid, yield 82%, mp: 187-188°C; ¹H-NMR (400 MHz, DMSO-*d*₆) δ: 2.04 (s, 6H, 2CH₃), 2.24 (s, 3H, CH₃), 2.25 (s, 3H, CH₃), 5.12 (s, 1H, Py-*H*), 5.47 (d, *J* = 1.64 Hz, 1H, Py-*H*), 6.95 (s, 2H, Ph-*H*), 7.06 (d, *J* = 8.24 Hz, 2H, Ph-*H*), 7.35 (d, *J* = 8.12 Hz, 2H, Ph-*H*), 8.43 (s, 1H, NH), 10.18 (s, 1H, CONH); ¹³C-NMR (100 MHz, DMSO-*d*₆) δ: 16.10, 20.79, 20.87, 83.76, 86.32, 120.02, 129.71, 129.89, 130.45,

130.89, 134.95, 138.61, 148.04, 154.03, 164.16, 168.11; ESI-MS: 335.5 [M+H]⁺.

4.1.6.3. 4-((4-(*mesityloxy*)-6-*oxo*-1,6-dihydropyridin-2-yl)amino)benzotrile (7c)

White solid, yield 82%, mp: 246-247°C; ¹H-NMR (400 MHz, DMSO-*d*₆) δ: 2.07 (s, 6H, CH₃), 2.34 (s, 3H, CH₃), 5.05 (d, *J* = 1.56 Hz, 1H, Py-*H*), 5.94 (d, *J* = 1.52 Hz, 1H, Py-*H*), 6.89 (s, 2H, Ph-*H*), 7.08 (d, *J* = 8.60 Hz, 2H, Ph-*H*), 7.51 (d, *J* = 8.52 Hz, 2H, Ph-*H*), 9.33 (s, 1H, NH), 11.11 (bs, 1H, CONH); ¹³C-NMR (100 MHz, DMSO-*d*₆) δ: 15.94, 20.84, 82.27, 89.68, 105.81, 118.85, 119.48, 129.65, 130.17, 133.63, 135.62, 143.20, 146.86, 147.50, 164.86, 170.94; MS-ESI: 346.3 [M+H]⁺.

4.1.6.4. 4-((6-((4-cyanophenyl)amino)-2-*oxo*-1,2-dihydropyridin-4-yl)oxy)-3,5-dimethylbenzotrile (7d)

White solid, yield 78%, decomposed at 250-252°C; ¹H-NMR (400 MHz, DMSO-*d*₆) δ: 2.15 (s, 6H, CH₃), 5.61 (d, *J* = 1.64 Hz, 1H, Py-*H*), 5.69 (d, *J* = 1.64 Hz, 1H, Py-*H*), 7.62 (d, *J* = 8.72 Hz, 2H, Ph-*H*), 7.72 (s, 2H, Ph-*H*), 7.83 (d, *J* = 8.72 Hz, 2H, Ph-*H*), 9.31 (s, 1H, NH), 10.56 (bs, 1H, CONH); ¹³C-NMR (100 MHz, DMSO-*d*₆) δ: 15.93, 87.35, 88.53, 101.63, 109.07, 117.97, 118.89, 120.21, 133.31, 133.43, 133.52, 146.27, 154.02, 155.07, 164.68, 166.43; MS-ESI: 357.3 [M+H]⁺.

4.1.6.5. 4-((4-(2,6-dimethylphenoxy)-6-*oxo*-1,6-dihydropyridin-2-yl)amino)benzotrile (7e)

White solid, yield 86%, mp: 182-184°C; ¹H-NMR (300 MHz, DMSO-*d*₆) δ: 2.09 (s, 6H, 2CH₃), 5.59 (d, *J* = 1.5 Hz, 1H, Py-*H*), 5.70 (d, *J* = 1.8 Hz, 1H, Py-*H*), 7.10-7.20 (m, 3H, Ph-*H*), 7.62 (d, *J* = 9.0 Hz, 2H, Ph-*H*), 7.82 (d, *J* = 9.0 Hz, 2H, Ph-*H*), 9.39 (s, 1H, NH); ¹³C-NMR (75 MHz, DMSO-*d*₆) δ: 15.69, 86.88, 88.14, 100.99, 117.45, 119.76, 125.74, 129.09, 130.42, 132.94, 145.85, 149.64, 154.30, 163.96, 166.98; ESI-MS: 332.5 [M+H]⁺.

4.1.6.6. 4-((4-(3,5-dimethylphenoxy)-6-*oxo*-1,6-dihydropyridin-2-yl)amino)benzotrile (7f)

White solid, yield 76%, mp: 246-248°C; ¹H-NMR (300 MHz, DMSO-*d*₆) δ: 2.29 (s, 6H, 2CH₃), 5.67 (d, *J* = 2.40 Hz, 1H, Py-*H*), 5.83 (d, *J* = 2.00 Hz, 1H, Py-*H*), 6.79 (s, 2H, Ph-*H*), 6.91 (s, 1H, Ph-*H*), 7.63 (d, *J* = 9.0 Hz, 2H, Ph-*H*), 7.85 (d, *J* = 9.0 Hz, 2H, Ph-*H*), 9.41 (s, 1H, NH), 10.56 (s, 1H, CONH); ¹³C-NMR (75 MHz, DMSO-*d*₆) δ: 20.74, 88.54, 90.08, 100.88, 117.35, 118.41, 119.79, 126.74, 132.93, 139.62, 145.93, 153.79, 154.25, 163.90, 167.87; ESI-MS: 332.5 [M+H]⁺.

4.1.7. General procedure for synthesis of

4-phenoxy-6-(phenylamino)pyridin-2(1H)-one derivatives 8(c-f)

Halogenated reagent (*N*-iodosuccinimide NIS, or *N*-bromosuccinimide NBS or *N*-chlorosuccinimide NCS) (1.2 mmol) was added to a solution of **7(c-f)** (1.0 mmol) in AcOH (4.0 mL) and CF₃COOH (2.2 mL). The mixture was stirred at room temperature until the starting reactant **7(c-f)** was completely consumed as detected by TLC. Then the mixture was poured into ice-water and neutralized with 28% aqueous NH₄OH. The resulting precipitate was separated by filtration, washed with ethyl acetate, and subsequently purified by flash column chromatography using ethyl acetate/petroleum ether (1:2) as eluent to give the product of **8(c-f)**.

4.1.7.1. 4-((5-iodo-4-(mesityloxy)-6-oxo-1,6-dihydropyridin-2-yl)amino)benzotrile (8c1)

Light yellow solid, yield 35%, decomposed at 254°C; ¹H-NMR (400 MHz, DMSO-*d*₆) δ: 2.04 (s, 6H, CH₃), 2.28 (s, 3H, CH₃), 5.43 (s, 1H, Py-*H*), 7.01 (s, 2H, Ph-*H*), 7.61 (d, *J* = 8.84 Hz, 2H, Ph-*H*), 7.82 (d, *J* = 8.72 Hz, 2H, Ph-*H*), 9.39 (s, 1H, NH), 11.34 (s, 1H, 1-NH); ¹³C-NMR (100 MHz, DMSO-*d*₆) δ: 16.11, 20.08, 83.68, 86.29, 119.97, 129.71, 129.90, 130.45, 130.86, 134.96, 138.63, 148.02, 154.02, 164.18, 168.09; MS-ESI: 472.3 [M+H]⁺.

4.1.7.2. 4-((5-bromo-4-(mesityloxy)-6-oxo-1,6-dihydropyridin-2-yl)amino)benzotrile (8c2)

White solid, yield 32%, mp: 130-132°C; ¹H-NMR (400 MHz, DMSO-*d*₆) δppm: 2.05 (s, 6H, CH₃), 2.28 (s, 3H, CH₃), 5.49 (s, 1H, Py-*H*), 7.01 (s, 2H, Ph-*H*), 7.60 (d, *J* = 8.76 Hz, 2H, Ph-*H*), 7.80 (d, *J* = 8.00 Hz, 2H, Ph-*H*), 9.37 (s, 1H, NH), 11.36 (s, 1H, 1-NH); ¹³C-NMR (100 MHz, DMSO-*d*₆) δppm: 15.97, 20.81, 101.75, 117.94, 120.18, 130.22, 130.24, 133.40, 135.51, 146.07, 148.27, 160.63, 163.08; MS-ESI: 424.5 [M+H]⁺.

4.1.7.3. 4-((5-chloro-4-(mesityloxy)-6-oxo-1,6-dihydropyridin-2-yl)amino)benzotrile (8c3)

White solid, yield 28%, mp: 144-146°C; ¹H-NMR (400 MHz, DMSO-*d*₆) δppm: 2.05 (s, 6H, CH₃), 2.28 (s, 3H, CH₃), 5.52 (s, 1H, Py-*H*), 7.02 (s, 2H, Ph-*H*), 7.60 (d, *J* = 8.88 Hz, 2H, Ph-*H*), 7.80 (s, 2H, Ph-*H*), 9.38 (s, 1H, NH), 11.38 (s, 1H, 1-NH); ¹³C-NMR (100 MHz, DMSO-*d*₆) δppm: 15.94, 20.81, 101.72, 117.87, 120.18, 130.22, 130.24, 133.40, 135.53, 146.09, 148.14, 159.65, 162.02; MS-ESI: 380.4 [M+H]⁺, 382.4 [M+H]⁺.

4.1.7.4. 4-((6-((4-cyanophenyl)amino)-3-iodo-2-oxo-1,2-dihydropyridin-4-yl)oxy)-3,5-

dimethylbenzotrile (8d1)

Light brown solid, yield 42%, decomposed at 235-236°C; ¹H-NMR (400 MHz, DMSO-*d*₆) δ: 2.15 (s, 6H, CH₃), 5.39 (s, 1H, Py-*H*), 7.60 (d, *J* = 8.76 Hz, 1H, Py-*H*), 7.76-7.80 (m, 4H, Ph-*H*), 9.30 (s, 1H, NH), 11.40 (bs, 1H, CONH); ¹³C-NMR (100 MHz, DMSO-*d*₆) δppm: 15.90, 101.93, 109.43, 118.08, 118.83, 120.13, 133.06, 133.43, 133.66, 145.87, 154.48, 163.49, 179.79; MS-ESI: 483.3 [M+H]⁺.

4.1.7.5. *4-((3-bromo-6-((4-nitrophenyl)amino)-2-oxo-1,2-dihydropyridin-4-yl)oxy)-3,5-dimethylbenzotrile (8d2)*

White solid, yield 28%, decomposed at 242-243°C; ¹H-NMR (400 MHz, DMSO-*d*₆) δppm: 2.14 (s, 6H, CH₃), 5.44 (s, 1H, Py-*H*), 7.63-7.98 (m, 5H, Ph-*H*), 9.39 (s, 1H, NH), 11.70 (bs, 1H, CONH); ESI-MS: 435.4 [M+H]⁺.

4.1.7.6. *4-((3-chloro-6-((4-nitrophenyl)amino)-2-oxo-1,2-dihydropyridin-4-yl)oxy)-3,5-dimethylbenzotrile (8d3)*

White solid, yield 34%, decomposed at 290°C; ¹H-NMR (400 MHz, DMSO-*d*₆) δppm: 2.15 (s, 6H, CH₃), 5.48 (s, 1H, Py-*H*), 7.62 (d, *J* = 8.56 Hz, 2H, Ph-*H*), 7.80 (s, 4H, Ph-*H*), 9.37 (s, 1H, NH), 11.56 (bs, 1H, CONH); ¹³C-NMR (100 MHz, DMSO-*d*₆) δppm: 15.76, 88.90, 93.66, 101.93, 109.43, 117.92, 118.80, 120.15, 133.08, 133.46, 133.73, 145.87, 154.05, 159.88, 160.87; ESI-MS: 391.3 [M+H]⁺.

4.1.7.7. *4-(((4-(2,6-dimethylphenoxy)-5-iodo-6-oxo-1,6-dihydropyridin-2-yl)amino)benzotrile (8e1)*

White solid, yield 36%, mp: 244-245°C; ¹H-NMR (300 MHz, DMSO-*d*₆) δ: 2.09 (s, 6H, 2CH₃), 5.43 (s, 1H, Py-*H*), 7.13-7.23 (m, 3H, Ph-*H*), 7.62 (d, *J* = 8.7 Hz, 2H, Ph-*H*), 7.82 (d, *J* = 9.0 Hz, 2H, Ph-*H*), 9.43 (s, 1H, NH), 11.35 (s, 1H, CONH); ¹³C-NMR (75 MHz, DMSO-*d*₆) δ: 15.67, 87.99, 101.20, 117.53, 119.71, 125.96, 129.19, 130.18, 132.91, 145.56, 150.24, 150.24, 162.79, 164.90; ESI-MS: 458.3 [M+H]⁺.

4.1.7.8. *4-(((5-bromo-4-(2,6-dimethylphenoxy)-6-oxo-1,6-dihydropyridin-2-yl)amino)benzotrile (8e2)*

White solid, yield 42%, mp: 240-241°C; ¹H-NMR (400 MHz, DMSO-*d*₆) δppm: 2.10 (s, 6H, 2CH₃), 5.49 (s, 1H, Py-*H*), 7.15-7.24 (m, 3H, Ph-*H*), 7.62 (d, *J* = 8.48 Hz, 2H, Ph-*H*), 7.82 (d, *J* = 8.20 Hz, 2H, Ph-*H*), 9.43 (s, 1H, NH), 11.46 (s, 1H, CONH); ¹³C-NMR (100 MHz, DMSO-*d*₆) δppm: 16.05, 82.52, 89.00, 101.78, 117.97, 120.18, 126.54, 129.75, 130.69, 133.41, 146.04, 150.46, 153.08, 160.68, 162.87; ESI-MS:

410.3 [M+H]⁺ .

4.1.7.9. 4-((5-chloro-4-(2,6-dimethylphenoxy)-6-oxo-1,6-dihydropyridin-2-yl)amino) benzonitrile (**8e3**)

White solid, yield 40%, mp: 260-261°C; ¹H-NMR (400 MHz, DMSO-*d*₆) δppm: 2.09 (s, 6H, 2CH₃), 5.48 (s, 1H, Py-*H*), 7.15-7.24 (m, 3H, Ph-*H*), 7.62 (d, *J* = 8.80 Hz, 2H, Ph-*H*), 7.81 (dd, *J* = 8.58 Hz, 2.92 Hz, 2H, Ph-*H*), 9.42 (s, 1H, NH), 11.43 (s, 1H, CONH); ¹³C-NMR (100 MHz, DMSO-*d*₆) δppm: 16.08, 88.72, 93.77, 101.76, 117.97, 120.19, 126.52, 129.73, 130.82, 133.41, 146.06, 150.55, 153.08, 160.76, 164.30; ESI-MS: 366.3 [M+H]⁺.

4.1.7.10. 4-((4-(3,5-dimethylphenoxy)-5-iodo-6-oxo-1,6-dihydropyridin-2-yl)amino) benzonitrile (**8f1**)

White solid, yield 36%, mp: 182-184°C; ¹H-NMR (400 MHz, DMSO-*d*₆) δ: 2.30 (s, 6H, 2CH₃), 5.67 (s, 1H, Py-*H*), 6.80 (s, 2H, Ph-*H*), 6.94 (s, 1H, Ph-*H*), 7.62 (d, *J* = 8.80 Hz, 2H, Ph-*H*), 7.81 (d, *J* = 7.92 Hz, 2H, Ph-*H*), 9.44 (s, 1H, NH), 11.39 (s, 1H, CONH); ¹³C-NMR (75 MHz, DMSO-*d*₆) δ: 21.24, 107.74, 118.04, 118.70, 120.22, 127.44, 133.46, 140.32, 146.05, 154.52, 163.28, 167.08; ESI-MS: 458.4 [M+H]⁺.

4.1.7.11. 4-((5-bromo-4-(3,5-dimethylphenoxy)-6-oxo-1,6-dihydropyridin-2-yl)amino) benzonitrile (**8f2**)

White solid, yield 32%, mp: 182-184°C; ¹H-NMR (300 MHz, DMSO-*d*₆) δppm: 2.30 (s, 6H, 2CH₃), 5.72 (s, 1H, Py-*H*), 6.95 (s, 1H, Ph-*H*), 6.82 (s, 2H, Ph-*H*), 6.05 (s, 1H, Py-*H*), 7.63 (d, *J* = 11.6 Hz, 2H, Ph-*H*), 7.82 (d, *J* = 11.6 Hz, 2H, Ph-*H*), 9.45 (s, 1H, NH), 11.46 (s, 1H, CONH); ¹³C-NMR (75 MHz, DMSO-*d*₆) δppm: 20.73, 90.83, 101.30, 117.47, 118.18, 119.69, 127.04, 132.95, 139.85, 145.52, 153.80, 160.17, 163.78; ESI-MS: 410.3 [M+H]⁺, 412.3 [M+H]⁺ .

4.1.7.12. 4-((5-chloro-4-(3,5-dimethylphenoxy)-6-oxo-1,6-dihydropyridin-2-yl)amino) benzonitrile (**8f3**)

White solid, yield 42%, mp: 200-202°C; ¹H-NMR (400 MHz, DMSO-*d*₆) δppm: 2.30 (s, 6H, 2CH₃), 5.75 (s, 1H, Py-*H*), 6.83 (s, 2H, Ph-*H*), 6.94 (s, 1H, Ph-*H*), 7.62 (d, *J* = 8.80 Hz, 2H, Ph-*H*), 7.79 (s, 2H, Ph-*H*), 9.42 (s, 1H, NH), 11.42 (s, 1H, CONH); ¹³C-NMR (100 MHz, DMSO-*d*₆) δppm: 21.23, 101.80, 117.92, 118.62, 120.17, 127.55, 133.45, 140.35, 146.05, 154.27, 159.72, 163.08; ESI-MS: 366.3 [M+H]⁺, 368.2 [M+H]⁺.

4.2. Biological activity evaluation

4.2.1 *In vitro* anti-HIV assay

The target compounds were evaluated for their activity against wild-type HIV-1 (strain HIV-III_B), double RT mutant strain HIV-1 III_B RES056 (RT K103N + Y181C) and HIV-2 (strain ROD) in MT-4 cells using the MTT method as previously described³². Briefly, stock solutions (10×final concentration) of test compounds were added in 25 µL volumes to two series of triplicate wells to allow simultaneous evaluation of their effects on mock- and HIV-infected cells at the beginning of each experiment. Serial five-fold dilutions of test compounds were made directly in flat-bottomed 96-well microtiter trays by adding 100 µL medium to the 25 µL stock solution and transferring 25 µL of this solution to another well that contained 100 µL medium using a Biomek 3000 robot (Beckman instruments, Fullerton, CA). Untreated control HIV- and mock-infected cell samples were included for each sample.

HIV-1(III_B)³³ or HIV-2 (ROD)³⁴ stock (50 µL) at 100-300 CCID₅₀ (50% cell culture infectious dose-50%) or culture medium was added to either the infected or mock-infected wells of the microtiter plate. Mock-infected cells were used to evaluate the effect of test compound on uninfected cells in order to assess the cytotoxicity of the test compound. Exponentially growing MT-4 cells were centrifuged for 5 min at 200 g and the supernatant was discarded. The MT-4 cells were resuspended at 6×10^5 cells/mL, and 50-µL volumes were transferred to the microtiter tray wells. Five days after infection, the viability of mock- and HIV-infected cells was examined spectrophotometrically by the MTT assay. The 50% cytotoxic concentration (CC₅₀) was defined as the concentration of the test compound that reduced the viability of the mock-infected MT-4 cells by 50%. The concentration achieving 50% protection against the cytopathic effect of the virus in infected cells was defined as the 50% effective concentration (EC₅₀).

4.2.2 HIV-1 RT inhibition assay

A RT assay kit produced by Roche was used for the RT inhibition assay. All the reagents for performing the RT reaction are contained in the kit and the ELISA procedures for RT inhibition assay was performed as described in the kit protocol.³⁵

³⁶

Briefly, the reaction mixture containing HIV-1 reverse transcriptase (RT) enzyme, reconstituted template and viral nucleotides [digoxigenin (DIG)-dUTP, biotin-dUTP and dTTP] in the incubation buffer with or without inhibitors was incubated for 1 h at

37 °C. Then, the reaction mixture was transferred to a streptavidine-coated microtitre plate (MTP) and incubated for another 1 h at 37 °C. The biotin-labeled dNTPs that was incorporated in cDNA chain in the presence of RT were bound to streptavidine. The unbound dNTPs were removed by rinsing using washing buffer followed by the addition of anti-DIG-POD working solution into the MTPs. After incubation for 1 h at 37 °C, the DIG-labeled dNTPs incorporated in cDNA were bound to the anti-DIG-POD antibody. The unbound anti-DIG-PODs were removed and the peroxide substrate (ABST) solution was added to the MTPs. Incubation of the reaction mixture at 25 °C until a green color was sufficiently developed for detection. The absorbance of the sample was determined at O.D. 405 nm using microtiter plate ELISA reader. The percentage inhibitory activity of RT inhibitors was calculated by formula as given below:

$$\% \text{Inhibition} = \frac{[\text{O.D. value with RT but without inhibitors} - \text{O.D. value with RT and inhibitors}]}{[\text{O.D. value with RT and inhibitors} - \text{O.D. value without RT and inhibitors}]^{35}}$$

The IC₅₀ values corresponded to the concentrations of the inhibitors required to inhibit biotin-dUTP incorporation by 50%.

4.3 Molecular Simulation

The molecules (**7d**, **8d1** and **TMC125**) for docking was optimized for 2000-generations until the maximum derivative of energy became 0.005kcal/(mol*Å), using the Tripos force field. Charges were computed and added according to Gasteiger - Huckel parameters. The published three-dimensional crystal structures of RT complexes with TMC125 (PDB code: 3MEC) were retrieved from the Protein Data Bank and were used for the docking studies by means of surflex-docking module of Sybyl-X 1.1. The protein was prepared by using the Biopolymer application accompanying Sybyl: The bound ligand was extracted from the complexes, water molecules were removed, hydrogen atoms were added, side chain amides and side chains bumps were fixed, and charges and atom types were assigned according to AMBER99. After the protomol was generated, the optimized compounds **7d**, **8d1** and **TMC125** were surflex-docked into the binding pocket of NNRTIs, with the relevant parameters set as defaults. The original ligand (TMC-125) of the coordinates (3MEC) was used as reference molecule to calculate the RMSD values. The docking scores related to binding affinities were calculated based on hydrophobic, polar, and

repulsive interactions as well as entropic effects and solvation. Top-scoring poses of **7d** were shown in overlap with the bound ligand (TMC-125) and the conformation of **8d1** in the binding site of RT respectively, by the software of PyMOL version 1.5 (<http://www.pymol.org/>). The secondary structure of RT are shown in cartoons, and only the key residues for interactions with the inhibitors were shown in sticks and labeled. The potential hydrogen-bondings were presented by dashed lines.

Conflict of interest

None.

Acknowledgments

We thank K. Erven, K. Uyttersprot and C. Heens for technical assistance with the anti-HIV assays. The financial support from the National Natural Science Foundation of China (NSFC No. 81273354, No. 81102320, No. 30873133, No. 30772629, No. 30371686), Key Project of NSFC for International Cooperation (No. 30910103908), Research Fund for the Doctoral Program of Higher Education of China (No. 20110131130005), Shandong Provincial Natural Science Foundation (No. ZR2009CM016) and KU Leuven (GOA 10/014) is gratefully acknowledged.

References

1. Sarafianos, S. G.; Marchand, B.; Das, K.; Himmel, D. M.; Parniak, M. A.; Hughes, S. H.; Arnold, E. *J. Mol. Biol.* **2009**, *385*, 693.
2. Sluis-Cremer, N.; Temiz, N. A.; Bahar, I. *Curr. HIV Res.* **2004**, *2*, 323.
3. Esnouf, R.; Ren, J.; Ross, C.; Jones, Y.; Stammers, D.; Stuart, D. *Nat. Struct. Mol. Biol.* **1995**, *2*, 303.
4. Zhan, P.; Chen, X.; Li, D.; Fang, Z.; De Clercq, E.; Liu, X. *Med. Res. Rev.* **2011**.
5. Li, D.; Zhan, P.; De Clercq, E.; Liu, X. *J. Med. Chem.* **2012**, *55*, 3595.
6. Waters, L.; John, L.; Nelson, M. *Int. J. Clin. Pract.* **2007**, *61*, 105.
7. Preston, B. D.; Poiesz, B. J.; Loeb, L. A. *Science* **1988**, *242*, 1168.
8. Zhang, Z.; Hamatake, R.; Hong, Z. *Antivir. Chem. Chemother.* **2004**, *15*, 121.
9. Ludovici, D. W.; De Corte, B. L.; Kukla, M. J.; Ye, H.; Ho, C. Y.; Lichtenstein, M. A.; Kavash, R. W.; Andries, K.; de Béthune, M.-P.; Azijn, H. *Bioorg. Med. Chem. Lett.* **2001**, *11*, 2235.
10. Azijn, H.; Tirry, I.; Vingerhoets, J.; de Béthune, M.-P.; Kraus, G.; Boven, K.; Jochmans, D.; Van Craenenbroeck, E.; Picchio, G.; Rimsky, L. T. *Antimicrob. Agents Chemother.* **2010**, *54*, 718.
11. Andries, K.; Azijn, H.; Thielemans, T.; Ludovici, D.; Kukla, M.; Heeres, J.; Janssen, P.; De Corte, B.; Vingerhoets, J.; Pauwels, R. *Antimicrob. Agents Chemother.* **2004**, *48*, 4680.
12. Chen, X.; Zhan, P.; Li, D.; De Clercq, E.; Liu, X. *Curr. Med. Chem.* **2011**, *18*, 359.
13. Mascolini, M. XVII International Drug Resistance Workshop: Fort Myers, Florida, **2009**.
14. Rimsky, L. T.; Azijn, H.; Tirry, I.; Vingerhoets, J.; Mersch, R.; Kraus, G.; de Béthune, M.-P.; Picchio, G.; Boyen, K. *Antiviral Ther.* **2009**, *14* (Suppl. 1), Abstract 120.
15. Anta, L.; Llibre, J. M.; Poveda, E.; Blanco, J. L.; Álvarez, M.; Pérez-Elías, M. J.; Aguilera, A.; Caballero, E.; Soriano, V.; de Mendoza, C. *AIDS* **2013**, *27*, 81.
16. Schrijvers, R. *Expert Opin. Pharmacother.* **2013**, *14*, 1087.
17. Putharoen, O.; Ruxrungham, K. *Future Virol.* **2013**, *8*, 113.
18. Benjahad, A.; Guillemont, J.; Andries, K.; Nguyen, C. H.; Grierson, D. S. *Bioorg. Med. Chem. Lett.* **2003**, *13*, 4309.
19. Guillemont, J. r. m.; Benjahad, A.; Oumouch, S.; Decrane, L.; Palandjian, P.; Vernier, D.; Queguiner, L.; Andries, K.; de Béthune, M.-P.; Hertogs, K. *J. Med. Chem.* **2009**, *52*, 7473.
20. Medina - Franco, J. L.; Martínez - Mayorga, K.; Juárez - Gordiano, C.; Castillo, R. *ChemMedChem* **2007**, *2*, 1141.
21. Benjahad, A.; Oumouch, S.; Guillemont, J.; Pasquier, E.; Mabire, D.; Andries, K.; Nguyen, C. H.; Grierson, D. S. *Bioorg. Med. Chem. Lett.* **2007**, *17*, 712.
22. Himmel, D. M.; Das, K.; Clark, A. D.; Hughes, S. H.; Benjahad, A.; Oumouch, S.; Guillemont, J.; Coupa, S.; Poncetlet, A.; Csoka, I. *J. Med. Chem.* **2005**, *48*, 7582.
23. Lansdon, E. B.; Brendza, K. M.; Hung, M.; Wang, R.; Mukund, S.; Jin, D.; Birkus, G.; Kutty, N.; Liu, X. *J. Med. Chem.* **2010**, *53*, 4295.
24. Viegas-Júnior, C.; Danuello, A.; da Silva Bolzani, V.; Barreiro, E. J.; Fraga, C. A. M. *Curr. Med. Chem.* **2007**, *14*, 1829.
25. Kaneko, C. U., K.; Sato, M.; Katagiri, N. *Chem. Pharm. Bull.* **1986**, *34*, 3658.
26. Ruggeri, S. G.; Vanderplas, B. C.; Anderson, B. G.; Breitenbach, R.; Urban, F. J.; Stewart, I., A Morgan; Young, G. R. *Org. Process Res. Dev.* **2008**, *12*, 411.
27. Kumar, V.; Dority, J. A.; Bacon, E. R.; Singh, B.; Leshner, G. Y. *J. Org. Chem.* **1992**, *57*, 6995.
28. Andries, K.; De Bethune, M.; Kukla, M.; Azijn, H.; Lewi, P.; Janssen, P.; Pauwels, R., 40th

- Interscience Conference on Antimicrobial Agents and Chemotherapy: Toronto, Canada, **2000**.
29. Das, K.; Clark, A. D.; Lewi, P. J.; Heeres, J.; de Jonge, M. R.; Koymans, L. M.; Vinkers, H. M.; Daeyaert, F.; Ludovici, D. W.; Kukla, M. J. *J. Med. Chem.* **2004**, *47*, 2550.
 30. Metrangolo, P.; Neukirch, H.; Pilati, T.; Resnati, G. *Accounts of chemical research* **2005**, *38*, 386.
 31. Lu, Y.; Liu, Y.; Xu, Z.; Li, H.; Liu, H.; Zhu, W. *Expert Opin. Drug Dis.* **2012**, *7*, 375.
 32. Pannecouque, C.; Daelemans, D.; De Clercq, E. *Nat. Protocols* **2008**, *3*, 427.
 33. Popovic, M.; Sarngadharan, M.; Read, E.; Gallo, R. *Science* **1984**, *224*, 497.
 34. Clavel, F.; Guetard, D.; Brun-Vezinet, F.; Chamaret, S.; Rey, M.; Santos-Ferreira, M.; Laurent, A.; Dauguet, C.; Katlama, C.; Rouzioux, C.; al., e. *Science* **1986**, *233*, 343.
 35. Rawal, R. K.; Tripathi, R.; Katti, S.; Pannecouque, C.; De Clercq, E. *Bioorg. Med. Chem.* **2007**, *15*, 1725.
 36. Rawal, R. K.; Tripathi, R.; Katti, S.; Pannecouque, C.; De Clercq, E. *Euro. J. Med. Chem.* **2008**, *43*, 2800.

Figure Captions

Fig. 1. Structures and anti-HIV-1 activities of DAPY and IOPY analogues^{22, 29}.

Fig. 2. Crystallographic overlays of TMC125 (purple) and R221239 (pink) with RT (performed by SYBYL-X 1.1, shown by PyMOL version 1.5; <http://www.pymol.org/>).

Fig. 3. The structure of novel 2-pyridone-typed NNRTIs designed by molecular hybridization of TMC-125 and R221239.

Fig. 4. The structural overlap of the most potent compound **7d** (blue) and TMC125 (orange) (Proposed hydrogen bonds are indicated with dashed lines in red. The docking result was performed by SYBYL-X 1.1, shown by PyMOL).

Fig. 5. The structural overlap of compound **7d** (blue) and 3-iodo-2-pyridone compound **8d1** (yellow) (Proposed hydrogen bonds are indicated with dashed lines in red. The docking result was performed by SYBYL-X 1.1, shown by PyMOL).

Scheme 1. Synthetic route of target compounds **6**, **7** and **8**. Reagents and conditions: (a) 30% H₂O₂, CF₃COOH, reflux; (b) POCl₃, reflux; (c) K₂CO₃, DMF, N₂, 100°C; (d) MeONa, MeOH, reflux; (e) Pd(OAc)₂, XantPhos, NaO-^tBu, N₂, 1,4-dioxane, 100°C; (f) TMSCl, NaI, CH₃CN, reflux; (g) NIS/NBS/NCS, AcOH, CF₃COOH, rt.

Table 1. *In vitro* anti-HIV-1 activity of 2-methoxypyridine derivatives **6(a-f)** and 2-pyridone derivatives **7(a-f)**.

Table 2. *In vitro* anti-HIV-1 activity of the 2-pyridone compounds with different substitutions (X) on the 3-position of the 2-pyridone ring.

Table 3. Inhibitory activity of representative 2-pyridone compounds against HIV-1 RT.

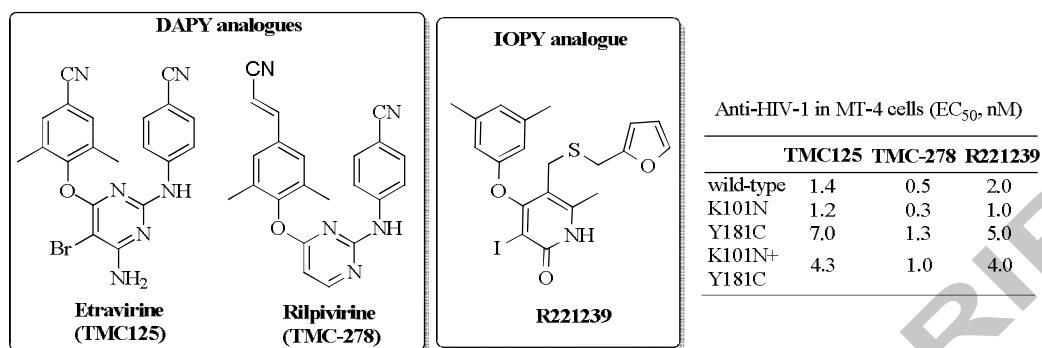


Fig. 1. Structures and anti-HIV-1 activities of DAPY and IOPY analogues [22, 23].

ACCEPTED MANUSCRIPT

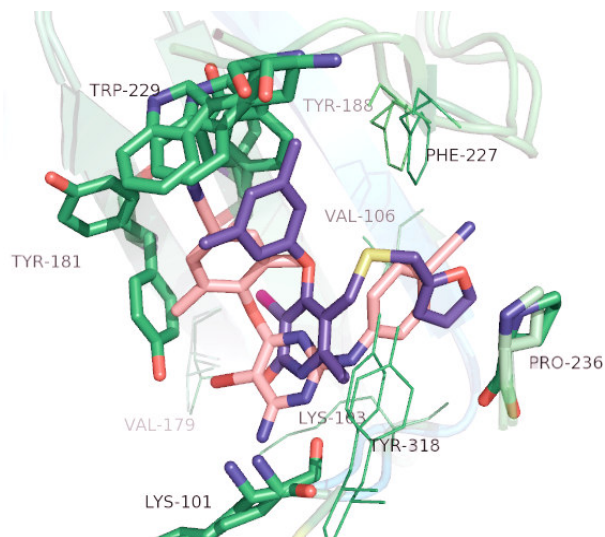


Fig. 2. Crystallographic overlay of TMC125 (purple) and R221239 (pink) with RT (performed by SYBYL-X 1.1, shown by PyMOL).

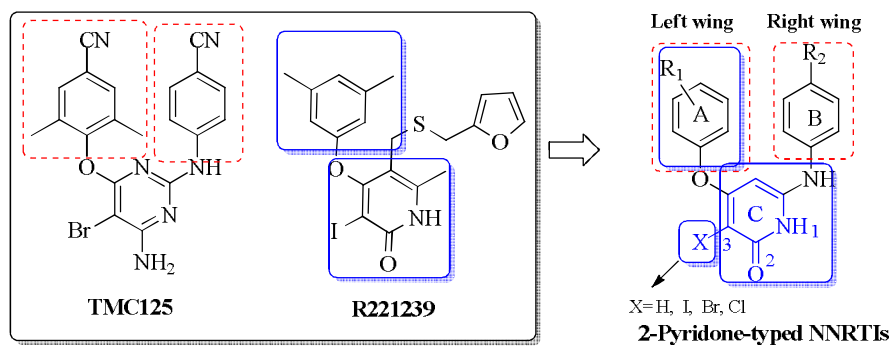


Fig. 3. Molecular hybridization of TMC-125 and R221239 to create the novel 2-pyridone-typed NNRTIs

ACCEPTED MANUSCRIPT

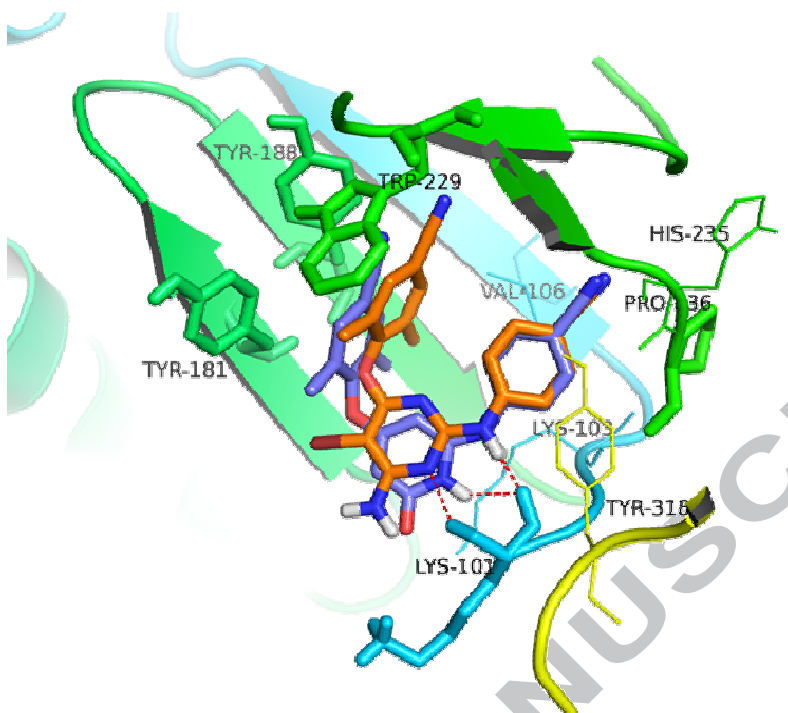


Fig. 4. The structural overlap of the most potent compound **7d** (blue) and TMC125 (orange) (Proposed hydrogen bonds are indicated with dashed lines in red. The docking result was performed by SYBYL-X 1.1, shown by PyMOL).

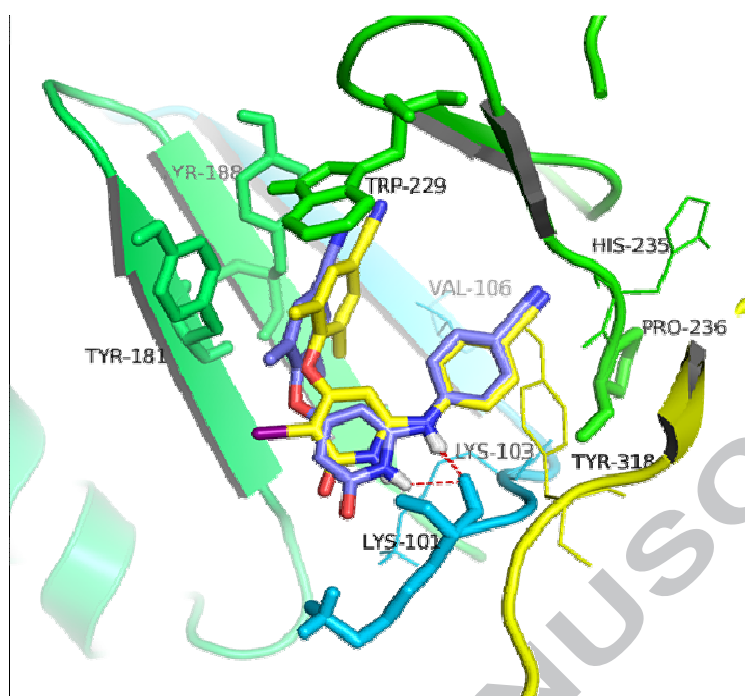
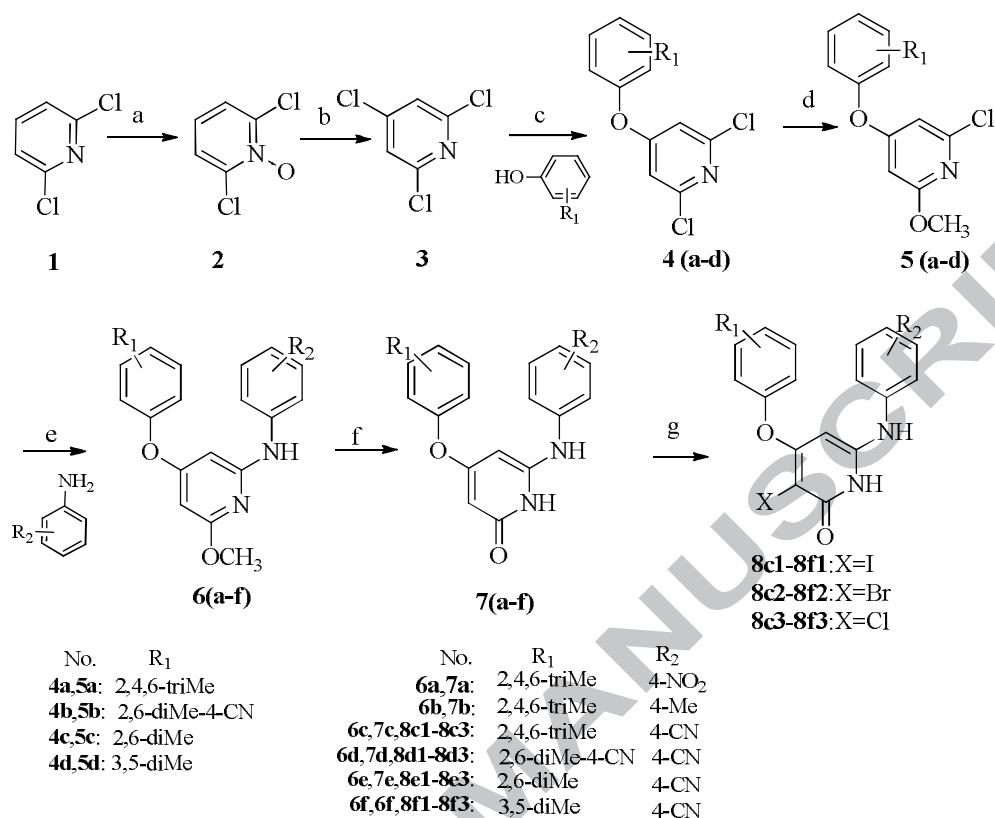
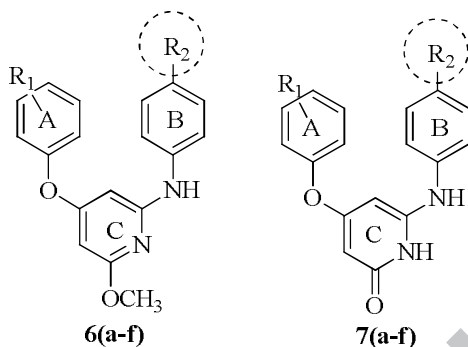


Fig. 5. The structural overlap of compound **7d** (blue) and 3-iodo-2-pyridone compound **8d1** (yellow) (Proposed hydrogen bonds are indicated with dashed lines in red. The docking result was performed by SYBYL-X 1.1, shown by PyMOL).



Scheme 1. Synthetic route of target compounds **6**, **7** and **8**. Reagents and conditions: (a) 30% H₂O₂, CF₃COOH, reflux; (b) POCl₃, reflux; (c) K₂CO₃, DMF, N₂, 100°C; (d) MeONa, MeOH, reflux; (e) Pd(OAc)₂, XantPhos, NaO^tBu, N₂, 1,4-dioxane, 100°C; (f) TMSCl, NaI, CH₃CN, reflux; (g) NIS/NBS/NCS, AcOH, CF₃COOH, rt.

Table 1. *In vitro* anti-HIV-1 activity of 2-methoxypyridine derivatives **6(a-f)** and 2-pyridone derivatives **7(a-f)**.



Compd.	R ₁	R ₂	EC ₅₀ ^a (μM)		CC ₅₀ ^b (μM)	SI ^c	
			III _B	RES056 ^e		III _B	RES056
6a	2,4,6-triMe	NO ₂	>7.2	nd ^d	7.2±1.5	<1	nd ^d
6b	2,4,6-triMe	CH ₃	>35	nd ^d	35±9.3	<1	nd ^d
6c	2,4,6-triMe	CN	0.84±0.43	>29	29±3	35	<1
6d	2,6-diMe-4-CN	CN	0.70±0.50	>147	>147	>211	-
6e	2,6-diMe	CN	>8.5	nd ^d	8.5±1.9	<1	nd ^d
6f	3,5-diMe	CN	>20	nd ^d	20±10	<1	nd ^d
7a	2,4,6-triMe	NO ₂	1.4±0.3	>26	26±3.5	19	<1
7b	2,4,6-triMe	CH ₃	1.4±0.4	>37	37±1.3	26	<1
7c	2,4,6-triMe	CN	0.37±0.10	>32	32±2.3	87	<1
7d	2,6-diMe-4-CN	CN	0.15±0.06	>25	25±1.5	166	<1
7e	2,6-diMe	CN	1.40±0.17	>36	36±2.3	26	<1
7f	3,5-diMe	CN	>46	nd ^d	46±5.1	<1	nd ^d
NVP			0.18±0.08	3.5	>15	>83	>4
DLV			0.91±0.05	>36	>36	>40	-

^a EC₅₀: concentration of compound required to achieve 50% protection of MT-4 cells against HIV-1-induced cytopathicity, as determined by the MTT method.

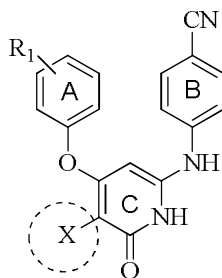
^b CC₅₀: concentration required to reduce the viability of mock-infected cells by 50%, as determined by the MTT method.

^c SI: selectivity index (CC₅₀/EC₅₀).

^d nd: not determined.

^e RES056: HIV-1 mutated strain bearing both K103N and Y181C mutations

Table 2. *In vitro* anti-HIV-1 activity of the 2-pyridone compounds with different substitutions (X) on the 3-position of the 2-pyridone ring.



Compd.	R ₁	X	EC ₅₀ ^a (μM)		CC ₅₀ ^b (μM)	SI ^c	
			III _B	RES056 ^e		III _B	RES056
8c1	2,4,6-triMe	I	5.6±0.6	>34	34±7.9	6	<1
8c2	2,4,6-triMe	Br	32±4.42	>294	>294	>9	X1
8c3	2,4,6-triMe	Cl	9.3±1.70	>329	>329	>35	X1
8d1	2,6-diMe-4-CN	I	2.9±0.59	>259	>259	>89	X1
8d2	2,6-diMe-4-CN	Br	1.2±0.28	>287	>287	>244	X1
8d3	2,6-diMe-4-CN	Cl	7.2±0.40	>319	>319	>44	X1
8e1	2,6-diMe	I	1.7±0.52	>2.8	28±2.6	16	<1
8e2	2,6-diMe	Br	3.6±3.2	>63	63±99	17	<1
8e3	2,6-diMe	Cl	2.4±0.89	>29	29±7.0	12	<1
8f1	3,5-diMe	I	>24	nd ^d	24±0.9	<1	nd ^d
8f2	3,5-diMe	Br	>19	nd ^d	19±3.8	<1	nd ^d
8f3	3,5-diMe	Cl	>21	nd ^d	21±1.9	<1	nd ^d
NVP			0.18±0.08	3.5	>15	>83	∞
DLV			0.91±0.05	>36	>36	>40	-

^a EC₅₀: concentration of compound required to achieve 50% protection of MT-4 cells against HIV-1-induced cytopathicity, as determined by the MTT method.

^b CC₅₀: concentration required to reduce the viability of mock-infected cells by 50%, as determined by the MTT method.

^c SI: selectivity index (CC₅₀/EC₅₀).

^d nd: not determined

^e RES056: HIV-1 mutated strain bearing both K103N and Y181C mutations

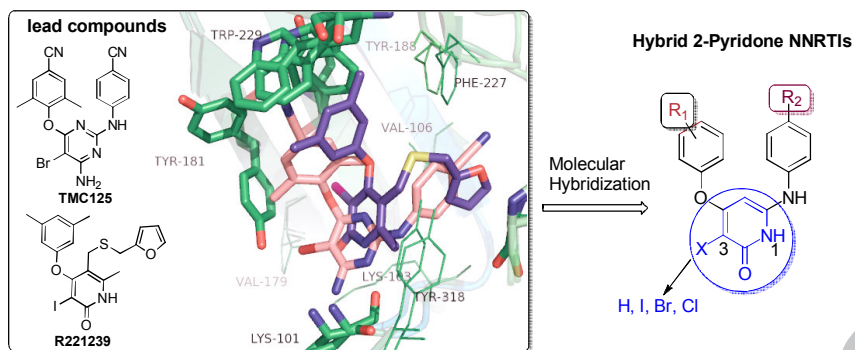
Table 3. Inhibitory activity of representative 2-pyridone compounds against HIV-1 RT.

Compd.	7d	7c	NVP	ETR
IC ₅₀ (μM) ^a	5.2	39	2.5	0.18

^a IC₅₀: Inhibitory concentration required to inhibit biotin deoxyuridine triphosphate (biotin-dUTP) incorporation into the HIV-1 RT by 50%.

ACCEPTED MANUSCRIPT

Graphical Abstract:



ACCEPTED MANUSCRIPT